The USTHB IGRF14 candidate models

M. Hamoudi[1], A. Lemgharbi[1, 2], and T. Amezza[1, 3]

[1] University of Sciences and Technology Houari Boumediène, USTHB, Algiers, Algeria.

[2] Tamanrasset Observatory, CRAAG, Tamanrasset, Algeria.

[3] Laboratoire de Physique Nucléaire et de Hautes Énergies Sorbonne Université, Paris, France

1. Introduction

This short report describes technical aspects of the derivation of the USTHB candidates for the IGRF-14.

There are three dedicated sections for the DGRF-2020, IGRF-2025 and SV-2025-2030, respectively. We have conducted various tests to estimate the robustness of our candidates, but these are not included in this report

2. DGRF 2020 technical description

2.1 Data

Our magnetic field model is built from SWARM level-1b satellite A data from 2019.0 to 2024.8,

2.2 Selection

The selection criteria used for these data are similar to those used by Lesur et al.(2008, 2010) and Mandea et al. (2012).

The satellite vector data are selected for magnetically quiet times according to the following criteria:

- Sampling points are separated by 30 seconds at minimum.

- Data are selected at local time between 23:00 and 05:00, with the sun below the horizon at 100 km above the Earth's reference radius (a = 6371.2km).

- Dst values should be in ±30nT and their time derivatives less than 100nT/day.

- Kp < 2

At all latitudes, i.e. polewards of ±55° latitude as well as mid-latitude, the three component vector magnetic data are used in North, East, Centre (NEC) system of coordinates.

- Data are selected at all local times, and independently of the sun position.

Only 357443 data points among 2,498,400 were retained for the inversions.

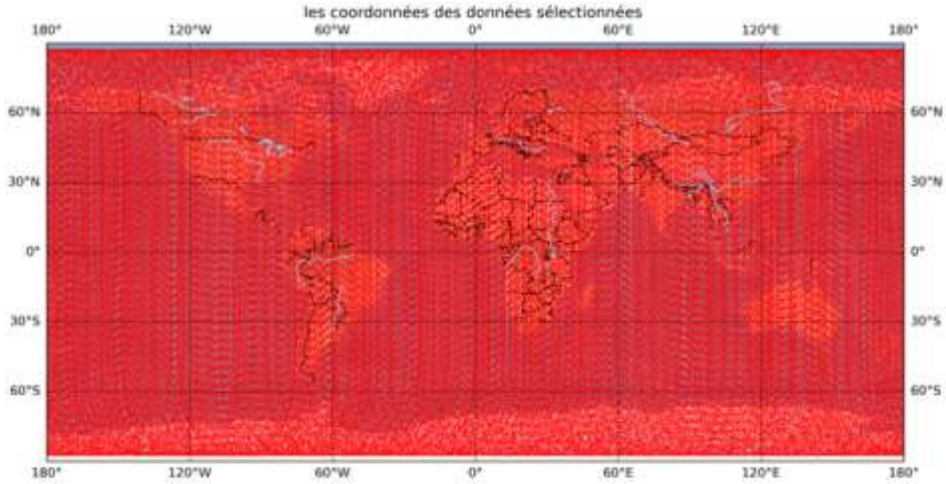

2.3 Mathematical Models:

Away from its sources, the magnetic field can be described as the negative gradient of potentials associated with sources of internal and external origin:

$$\vec{B} = -\overrightarrow{\nabla V} \Longrightarrow \begin{cases} B_\theta = \dfrac{-1}{r}\dfrac{\partial}{\partial\theta}(V) \\ B_\varphi = \dfrac{-1}{rsin\theta}\dfrac{\partial}{\partial\varphi}(V) \\ B_r = \dfrac{-\partial}{\partial\theta}(V) \end{cases}$$

θ, φ, r and a are the co-latitude, longitude, satellite altitude and model reference radius, respectively, in geocentric coordinates.

The geocentric components are given in close form below:

$$
\begin{aligned}
B_\theta(r,\theta,\varphi,t) = &-\sum_{l=1}^{13}\left(\frac{a}{r}\right)^{l+2}\sum_{m=-1}^{1} g_l^m \frac{\partial}{\partial\theta} Y_l^m(\theta,\varphi) \\
&-\sum_{l=1}^{13}\left(\frac{a}{r}\right)^{l+2}(t-t_0)\sum_{m=-1}^{1} g_l^m \frac{\partial}{\partial\theta} Y_l^m(\theta,\varphi) \\
&-\sum_{l=14}^{30}\left(\frac{a}{r}\right)^{l+2}\sum_{m=-1}^{1} g_l^m \frac{\partial}{\partial\theta} Y_l^m(\theta,\varphi) \\
&-\sum_{l=1}^{13}\left(\frac{a}{r}\right)^{l+2} I_{st}(t)\sum_{m=-1}^{1} g_l^m \frac{\partial}{\partial\theta} Y_l^m(\theta,\varphi) - \sum_{l=1}^{1}\left(\frac{r}{a}\right)^{l}\sum_{m=-1}^{1} q_l^m \frac{\partial}{\partial\theta} Y_l^m(\theta,\varphi) \\
&-\sum_{l=1}^{1}\left(\frac{r}{a}\right)^{l} E_{st}(t)\sum_{m=-1}^{1} q_l^m \frac{\partial}{\partial\theta} Y_l^m(\theta,\varphi)
\end{aligned}
$$

$$
\begin{aligned}
B_\varphi(r,\theta,\varphi,t) = &-\sum_{l=1}^{13}\left(\frac{a}{r}\right)^{l+2}\sum_{m=-1}^{1} g_l^m \frac{1}{sin\theta}\frac{\partial}{\partial\varphi} Y_l^m(\theta,\varphi) \\
&-\sum_{l=1}^{13}\left(\frac{a}{r}\right)^{l+2}(t-t_0)\sum_{m=-1}^{1} g_l^m \frac{1}{sin\theta}\frac{\partial}{\partial\varphi} Y_l^m(\theta,\varphi) \\
&-\sum_{l=14}^{30}\left(\frac{a}{r}\right)^{l+2}\sum_{m=-1}^{1} g_l^m \frac{1}{sin\theta}\frac{\partial}{\partial\varphi} Y_l^m(\theta,\varphi) \\
&-\sum_{l=1}^{13}\left(\frac{a}{r}\right)^{l+2} I_{st}(t)\sum_{m=-1}^{1} g_l^m \frac{1}{sin\theta}\frac{\partial}{\partial\varphi} Y_l^m(\theta,\varphi) \\
&-\sum_{l=1}^{1}\left(\frac{r}{a}\right)^{l}\sum_{m=-1}^{1} q_l^m \frac{1}{sin\theta}\frac{\partial}{\partial\varphi} Y_l^m(\theta,\varphi) \\
&-\sum_{l=1}^{1}\left(\frac{r}{a}\right)^{l} E_{st}(t)\sum_{m=-1}^{1} q_l^m \frac{1}{sin\theta}\frac{\partial}{\partial\varphi} Y_l^m(\theta,\varphi)
\end{aligned}
$$

$$
\begin{aligned}
B_r(r,\theta,\varphi,t) = &\sum_{l=1}^{13}(l+1)\left(\frac{a}{r}\right)^{l+2}\sum_{m=-1}^{1} g_l^m Y_l^m(\theta,\varphi) \\
&+ \sum_{l=1}^{13}(l+1)\left(\frac{a}{r}\right)^{l+2}(t-t_0)\sum_{m=-1}^{1} g_l^m Y_l^m(\theta,\varphi) \\
&+ \sum_{l=14}^{30}(l+1)\left(\frac{a}{r}\right)^{l+2}\sum_{m=-1}^{1} g_l^m Y_l^m(\theta,\varphi) \\
&+ \sum_{l=1}^{13}(l+1)\left(\frac{a}{r}\right)^{l+2} I_{st}(t)\sum_{m=-1}^{1} g_l^m Y_l^m(\theta,\varphi) \\
&- \sum_{l=1}^{1} l\left(\frac{r}{a}\right)^{l-1}\sum_{m=-1}^{1} q_l^m Y_l^m(\theta,\varphi) - \sum_{l=1}^{1} l\left(\frac{r}{a}\right)^{l-1} E_{st}(t)\sum_{m=-1}^{1} q_l^m Y_l^m(\theta,\varphi)
\end{aligned}
$$

Where the Schmidt semi-normalized spherical harmonics $Y_l^m$and their derivatives,may be written as follows :

$$
Y_l^m(\theta,\varphi) = \begin{cases} cos(m\varphi)P_l^m(cos\theta) m > 0 \\ sin(m\varphi)P_l^m(cos\theta) m < 0 \end{cases}
$$

$$
\frac{\partial}{\partial\theta}Y_l^m(\theta,\varphi) = \begin{cases} cos(m\varphi)\frac{\partial}{\partial\theta}P_l^m(cos\theta) m > 0 \\ s \in (m\varphi)\frac{\partial}{\partial\theta}P_l^m(cos\theta) m < 0 \end{cases}
$$

$$
\frac{\partial}{\partial\varphi}Y_l^m(\theta,\varphi) = \begin{cases} \frac{-m}{sin\theta} sin(m\varphi)P_l^m(cos\theta) m > 0 \\ \frac{m}{sin\theta} cos(m\varphi)P_l^m(cos\theta) m < 0 \end{cases}
$$

We know that the Geographical components of the magnetic field are related to Geocentric ones through :

$X = -B_\theta$

$Y = B_\varphi$

$Z = -B_r$

Which gives:

$$
\begin{aligned}
X = {} & \sum_{l=1}^{13} \left(\frac{a}{r}\right)^{l+2} \sum_{m=-1}^{1} g_l^m \frac{\partial}{\partial\theta} Y_l^m(\theta,\varphi) + \sum_{l=1}^{13} \left(\frac{a}{r}\right)^{l+2} (t-t_0) \sum_{m=-1}^{1} g_l^m \frac{\partial}{\partial\theta} Y_l^m(\theta,\varphi) \\
& + \sum_{l=14}^{30} \left(\frac{a}{r}\right)^{l+2} \sum_{m=-1}^{1} g_l^m \frac{\partial}{\partial\theta} Y_l^m(\theta,\varphi) \\
& + \sum_{l=1}^{13} \left(\frac{a}{r}\right)^{l+2} I_{st}(t) \sum_{m=-1}^{1} g_l^m \frac{\partial}{\partial\theta} Y_l^m(\theta,\varphi) + \sum_{l=1}^{1} \left(\frac{r}{a}\right)^{l} \sum_{m=-1}^{1} q_l^m \frac{\partial}{\partial\theta} Y_l^m(\theta,\varphi) \\
& + \sum_{l=1}^{1} \left(\frac{r}{a}\right)^{l} E_{st}(t) \sum_{m=-1}^{1} q_l^m \frac{\partial}{\partial\theta} Y_l^m(\theta,\varphi)
\end{aligned}
$$

$$
\begin{aligned}
Y = {} & -\sum_{l=1}^{13} \left(\frac{a}{r}\right)^{l+2} \sum_{m=-1}^{1} g_l^m \frac{1}{sin\theta} \frac{\partial}{\partial\varphi} Y_l^m(\theta,\varphi) \\
& - \sum_{l=1}^{13} \left(\frac{a}{r}\right)^{l+2} (t-t_0) \sum_{m=-1}^{1} g_l^m \frac{1}{sin\theta} \frac{\partial}{\partial\varphi} Y_l^m(\theta,\varphi) \\
& - \sum_{l=14}^{30} \left(\frac{a}{r}\right)^{l+2} \sum_{m=-1}^{1} g_l^m \frac{1}{sin\theta} \frac{\partial}{\partial\varphi} Y_l^m(\theta,\varphi) \\
& - \sum_{l=1}^{13} \left(\frac{a}{r}\right)^{l+2} I_{st}(t) \sum_{m=-1}^{1} g_l^m \frac{1}{sin\theta} \frac{\partial}{\partial\varphi} Y_l^m(\theta,\varphi) \\
& - \sum_{l=1}^{1} \left(\frac{r}{a}\right)^{l} \sum_{m=-1}^{1} q_l^m \frac{1}{sin\theta} \frac{\partial}{\partial\varphi} Y_l^m(\theta,\varphi) \\
& - \sum_{l=1}^{1} \left(\frac{r}{a}\right)^{l} E_{st}(t) \sum_{m=-1}^{1} q_l^m \frac{1}{sin\theta} \frac{\partial}{\partial\varphi} Y_l^m(\theta,\varphi)
\end{aligned}
$$

$$
\begin{aligned}
Z = {} & -\sum_{l=1}^{13} (l+1) \left(\frac{a}{r}\right)^{l+2} \sum_{m=-1}^{1} g_l^m Y_l^m(\theta,\varphi) - \sum_{l=1}^{13} (l+1) \left(\frac{a}{r}\right)^{l+2} (t-t_0) \sum_{m=-1}^{1} g_l^m Y_l^m(\theta,\varphi) \\
& - \sum_{l=14}^{30} (l+1) \left(\frac{a}{r}\right)^{l+2} \sum_{m=-1}^{1} g_l^m Y_l^m(\theta,\varphi) \\
& - \sum_{l=1}^{13} (l+1) \left(\frac{a}{r}\right)^{l+2} I_{st}(t) \sum_{m=-1}^{1} g_l^m Y_l^m(\theta,\varphi) \\
& + \sum_{l=1}^{1} l \left(\frac{r}{a}\right)^{l-1} \sum_{m=-1}^{1} q_l^m Y_l^m(\theta,\varphi) + \sum_{l=1}^{1} l \left(\frac{r}{a}\right)^{l-1} E_{st}(t) \sum_{m=-1}^{1} q_l^m Y_l^m(\theta,\varphi)
\end{aligned}
$$

We have modeled the internal and external magnetic fields by considering expansion degrees:

Core field: N_{core}= 13

Secular variation: N_{sv}= 13

Lithospheric field: N_{lith}= 30

Induced field: N_{ind}= 1

External field: N_{extern}= 1

Parameterization of the Models

One have to solve the equation given below to derive the internal and external models g_l^m and q_l^m.

$$m = (A^t C_e^{-1} A + \lambda C_m^{-1})^{-1} (A^t C_e^{-1} d)$$

where :

A is an N x M matrix of coefficients, independent of data values and model parameters

C_e^{-1}: Diagonal Matrix with $\frac{1}{\sigma^2}$ elements

C_m^{-1}: Indentity Matrix with 1/25 for diagonal elements.

$$m \quad = (A^t C_e^{-1} A + \lambda C_m^{-1})^{-1} (A^t C_e^{-1} d + \lambda C_m^{-1} m_0)$$

In our computation, we consider:

C_m^{-1}: 1/25 for the diagonal elements

m_0: Modèle IGRF-20

λ= 0.25

3. Results

3.1 DGRF candidate

The DGRF candidate is the average model 2020.0 of 2020.5 and 2019.5 models

3.2 IGRF candidate

The IGRF candidate is model derived with data spanning the period 2023.0 to 2024.8

3.3 IGRF-SV for 2025-2030 candidate

The secular variation model is jointly derived with the IGRF model assuming linear variation of the coefficients $\dot{g}_n^m$ and $\dot{h}_n^m$ during the five years interval 2025-2030

No uncertainties estimates have been provided for the coefficients